Solid-State Electronics Vol. 31, No. 11, pp. 1587–1594, 1988
Printed in Great Britain.

0038-1101/88 $3.00 + 0.00

ANALYSIS OF CHARGE-COLLECTION EFFICIENCY MEASUREMENTS IN SCHOTTKY DIODES

C. Donolato
CNR-Istituto LAMEL, Via Castagnoli 1, 40126 Bologna, Italy

(*Received* 2 *March* 1988)

Abstract—A simplified method is described to evaluate the minority-carrier diffusion length L from electron beam induced current measurements in Schottky diodes at normal irradiation. The method relies on the analysis of the high-energy part of the plot of the charge-collection efficiency η of the device vs the primary electron range R, on the basis of approximate theoretical expressions valid for large R. For a known depletion layer width, the value of L and the associated error are obtained by a single parameter fit, independently of the value of the metallization thickness. Very small values of L can be estimated directly from the maximum of the plot of $R\eta$ vs R. The applicability of the new procedure is illustrated by evaluating data available from the literature on GaAs and Si.

1. INTRODUCTION

The minority-carrier diffusion length in a semiconductor can be determined by electron beam excitation using a number of geometries[1]. In the configuration introduced by Wu and Wittry[2], the electron beam is incident normally to the semiconductor surface, where a Schottky diode with a thin metallization has been formed (Fig. 1). By measuring the ratio between the beam-induced current and the total generation rate, one obtains the fraction of the beam-injected charge that is collected by the Schottky barrier, i.e. the charge-collection efficiency η of the device. The determination of η as a function of the electron beam energy E yields a plot $\eta(E)$, which contains the information about the diffusion length L. This configuration offers the advantage of allowing the measurement of local values of L and is also not affected by the surface properties of the semiconductor.

Usually, to extract the value of L from collection efficiency measurements, theoretical $\eta(E)$ curves are compared to the experimental ones. This fitting procedure involves as unknown paramaters L and the thickness h of the metal layer; the width W of the depletion region is more often assumed to be known independently[2,3], but sometimes is regarded as an additional parameter of the fit[4].

However, it has been observed that the value of L chiefly affects the high-energy portion of the $\eta(E)$ curve[2], so that it appears reasonable to attempt to determine L using high-energy data only. The expected advantages of this procedure are a simplification of the theoretical expressions of $\eta(E)$ in the limit of large E and an easier evaluation of L by a single-parameter fit to experiment.

In this study, such expressions are derived and applied to the graphical or numerical evaluation of charge-collection efficiency data. The practicability of the new evaluation techniques is demonstrated by applying them to published experimental measurements performed both on GaAs and Si.

2. THE MODEL

2.1. Theory

Because of the planar symmetry, the treatment of charge-collection in the device of Fig. 1 can be 1-D and involves only the depth coordinate z. Let $\phi(z)$ be the charge-collection probability in the device, i.e. the probability that a carrier generated at a depth z will be collected, and $g(z, E)$ [$\text{cm}^{-1}\,\text{s}^{-1}$] the normalized, energy-dependent, depth distribution of the electron beam generation in the semiconductor. The charge-collection efficiency $\eta(E)$ is then given by[5]:

$$\eta(E) = \int_0^\infty \phi(z) g(z, E)\,dz. \qquad (1)$$

It has been shown that $g(z, E)$ can be expressed through a function Λ of the single variable $\zeta = z/R$,

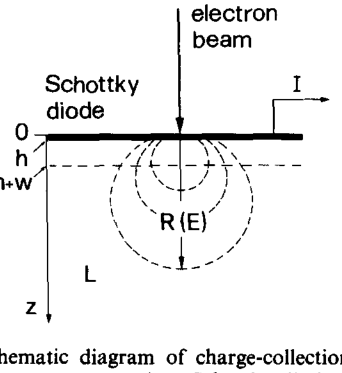

Fig. 1. Schematic diagram of charge-collection efficiency measurements in a Schottky diode.

where $R = R(E)$ is the range of primary electrons in the semiconductor at the energy E; the pertinent expression for Λ has been given by Wu and Wittry[2] for GaAs and by Everhart and Hoff[6] for Si. Thus eqn (1) can be written in general as:

$$\eta(R) = \frac{1}{R}\int_0^\infty \phi(z)\Lambda(z/R)\,dz. \quad (2)$$

According to the usual models for $\phi(z)$[2,5], it is assumed that $\phi(z) = 0$ for $0 \leqslant z \leqslant h$, where h is the thickness of the metal layer (or the equivalent thickness, if the density or the atomic number of the metal and semiconductor are very different). In the depletion layer $h < z \leqslant h + W$ complete collection, i.e. $\phi(z) = 1$ is assumed; in the bulk of the semiconductor $z > h + W$, $\phi(z) = \exp[-(z - h - W)/L]$. With this specification, and introducing the variable ζ, eqn (2) becomes:

$$\eta(R) = \int_{h/R}^{(h+W)/R} \Lambda(\zeta)\,d\zeta + \exp[(h+W)/L] \times \int_{(h+W)/R}^{\infty} \exp(-R\zeta/L)\Lambda(\zeta)\,d\zeta. \quad (3)$$

The values of h, L and possibly of W are usually obtained by fitting to experiment this expression, with a proper choice of Λ.

The attempt made here is to find an approximation to eqn (3) for large values of R, i.e. for $R \gg h + W$, and to use this approximation for evaluating the high-energy $\eta(R)$ data. Thus the lower limit of the first integral in eqn (3) can be replaced by 0, by simultaneously subtracting the additional contribution of the interval $(0, h/R)$, which is approximately $h\Lambda(0)/R$. The second integral over the range $[(h + W)/R, \infty]$ can be written as the difference between two integrals over $(0, \infty)$ and $[0, (h + W)/R]$. Hence:

$$\eta(R) \simeq -(h/R)\Lambda(0) + \exp[(h+W)/L] \times \int_0^\infty \exp(-R\zeta/L)\Lambda(\zeta)\,d\zeta - \int_0^{(h+W)/R} \Lambda(\zeta) \times \{\exp[-(R\zeta - h - W)/L] - 1\}\,d\zeta. \quad (4)$$

We may evaluate approximately the second integral of eqn (4) by observing that the smooth function $\Lambda(\zeta)$ changes little in the small interval $[0, (h + W)/R]$, and can therefore be approximated by $\Lambda(0)$. Thus:

$$\eta(R) \simeq -(h/R)\Lambda(0) + \exp[(h+W)/L]\eta_0(R) - \Lambda(0) \times \int_0^{(h+W)/R} \{\exp[-(R\zeta - h - W)/L] - 1\}\,d\zeta, \quad (5)$$

where

$$\eta_0(R) = \int_0^\infty \exp(-R\zeta/L)\Lambda(\zeta)\,d\zeta \quad (6)$$

represents the collection efficiency of an ideal surface barrier with $h = W = 0$. The value of the integral in eqn (5) is $(L/R)\{\exp[(h + W)/L] - (h + W)/L - 1\}$; since usually $(h + W)/L < 1/3$ (higher resistivity materials, where W is larger have also larger L; see e.g. Table 1), this expression can be approximated to the second order of $(h + W)/L$ by $\frac{1}{2}(h + W)^2/(RL)$. Hence:

$$\eta(R) \simeq -\Lambda(0)[h/R + \tfrac{1}{2}(h+W)^2/(RL)] + \exp[(h+W)/L]\eta_0(R). \quad (7)$$

We may reduce this expression further by estimating the relative weight of its terms. It is convenient to consider separately the two cases where, in the high-energy interval examined, $L \ll R$ or $L \gtrsim R$.

When $L \ll R$, the value of $\eta_0(R)$ can be estimated through the leading term of its asymptotic expansion with respect to $R/L \gg 1$, which is $\Lambda(0)L/R$. Since $(h + W)/L < 1/3$, we can approximate the exponential in eqn (7) by $1 + (h + W)/L$. Thus:

$$\eta(R) \simeq -\tfrac{1}{2}\Lambda(0)(h+W)^2/(RL) + (1 + W/L)\Lambda(0)L/R, \quad (8)$$

where the term $-\Lambda(0)h/R$ of eqn (7) has cancelled out with an opposite contribution arising from the term involving η_0. The ratio of the first addend of eqn (8) to the second one is $\frac{1}{2}(h + W)^2/L^2 < 1/18$. Therefore, with a relative error less than $\sim 5\%$ we can simplify eqn (7) to:

$$\eta(R) \simeq \exp(W/L)\eta_0(R); \quad R \gg h + W,\ L \ll R. \quad (9)$$

If $L \gtrsim R$, being $(h + W)/R \ll 1$ we also have $(h + W)/L \ll 1$. Keeping only first-order terms, with some rearrangement, eqn (7) can be written as:

$$\eta(R) \simeq -\Lambda(0)h/R + (h/L)\eta_0(R) + (1 + W/L)\eta_0(R). \quad (10)$$

Since $L \gtrsim R$, the sum of the first two terms of this equation is less than, or about equal to $(h/R)\cdot[-\Lambda(0) + \eta_0(R)]$. In addition, $\Lambda(0)$ and $\eta_0(R)$ (for $R/L \lesssim 1$) are both of the order of magnitude of unity (see later), therefore we may write with a relative error less than h/R:

$$\eta(R) \simeq (1 + W/L)\eta_0(R); \quad R \gg h + W,\ L \gtrsim R, \quad (11)$$

which is the same as eqn (9), being here $W/L \ll 1$. In conclusion, the approximation for η of eqn (9) holds, in the limit of $(h + W)/R \ll 1$, for any L larger than $3\cdot(h + W)$, though with better accuracy in the case of long diffusion lengths.

The peculiar structure of eqn (9) brings an advantage, which can be better seen by taking the logarithm:

$$\ln \eta(R) \simeq W/L + \ln \eta_0(R/L). \quad (12)$$

Equation (12) shows that in the high-energy region the semi-logarithmic η vs R curves for a given value of L, but different W, are identical in shape but shifted vertically over a distance W/L with respect to the reference curve with $W = 0$. This property suggests an easy graphical method of estimating the value of L from high-energy $\eta(R)$ data.

A family of theoretical curves of $\ln \eta_0$ vs R for different values of L is drawn on a transparent sheet, which is superimposed on a similar (i.e. with the same semilogarithmic scale) plot of the experimental $\eta(R)$ data. The best-fit theoretical curve is then selected by shifting upwards the template with respect to the experimental plot. The amount of this translation, according to eqn (12), is W/L and should therefore be consistent with the (even roughly) known value of W and the value of L that labels the best-fit curve. Consistency is obtained by trial and error; the estimate of L obtained by this procedure can be refined by numerical fitting, as illustrated in the next section.

2.2. Fit to experiment

The experimental data typically consists of N values of the collection efficiency y_i obtained at $R_i = R(E_i)$, and are to be fitted with the model function [see eqn (9)]:

$$\eta(R, L, W) = \exp(W/L)\eta_0(R/L), \tag{13}$$

with η_0 given by eqn (6). Since W is considered here as known, the required fit involves only L, though not in a linear way. Let us write the model function of eqn (13) as $\eta(R, \lambda)$, with $\lambda = 1/L$. A best fit in the least-squares sense requires the minimization with respect to λ of:

$$V(\lambda) = \sum_{i=1}^{N} [y_i - \eta(R_i, \lambda)]^2. \tag{14}$$

This nonlinear problem can be converted to a linear one[7] by writing $\lambda = \lambda_0 + \epsilon$, where λ_0 is a starting value of λ, possibly obtained with the graphical procedure described in the previous paragraph, and ϵ is a correction to be determined. According to the Gauss–Newton method[8], the model function is then approximated by its linear expansion about λ_0:

$$\eta(R_i, \lambda) \simeq \eta(R_i, \lambda_0) + \left.\frac{\partial \eta}{\partial \lambda}\right|_{\lambda=\lambda_0} \cdot \epsilon = \eta_i^0 + g_i^0 \epsilon. \tag{15}$$

The values of η_i^0 and g_i^0 can be calculated using the expressions for η_0 and $d\eta_0/d\rho$ of Sections 3.1, 3.3 and eqn (13). Substituting eqn (15) into eqn (14), it is easy to find that the solution of the linearized problem is given by:

$$\epsilon_0 = \sum_{i=1}^{N} (y_i - \eta_i^0) g_i^0 \Big/ \sum_{i=1}^{N} (g_i^0)^2. \tag{16}$$

The resulting value of λ is $\lambda_1 = \lambda_0 + \epsilon_0$, which is then used as a starting value of a new Taylor's expansion to yield a new correction ϵ_1. At each iteration the value of $V(\lambda)$ is computed to check that the minimum is being approached. The procedure is repeated until the change in λ between successive steps becomes small in comparison to its standard deviation, which is estimated as explained shortly. The last-step value λ_{k+1} yields the best fit value of the diffusion length $\hat{L} = 1/\hat{\lambda} = 1/\lambda_{k+1}$.

An estimate of the error by which this determination of L is affected, as a consequence of the scatter of the values y_i about the best-fit curve, can be obtained by analogy with the linear regression, although the related arguments are expected to hold here only approximately[8,9]. Thus assuming that the y_i's are random variables normally distributed about $\eta(R_i, \hat{\lambda})$ with common variance σ^2, we may estimate σ^2 by[8]:

$$s^2 = \frac{1}{N-1} \sum_{i=1}^{N} [y_i - \eta(R_i, \hat{\lambda})]^2. \tag{17}$$

By treating λ_k as a non-random variable[7, 9], we have:

$$\sigma^2(\hat{\lambda}) = \sigma^2(\lambda_k + \epsilon_k) = \sigma^2(\epsilon_k). \tag{18}$$

Writing eqn (16) at λ_k yields:

$$\epsilon_k = \sum_{i=1}^{N} (y_i - \eta_i^k) g_i^k \Big/ \sum_{i=1}^{N} (g_i^k)^2. \tag{19}$$

Since η_i^k will be close enough to $\eta_i^{k+1} = \eta(R_i, \hat{\lambda})$, $y_i - \eta_i^k$ will also be approximately normally distributed with mean zero and variance σ^2; hence:

$$\sigma^2(\epsilon_k) = \sigma^2 \Big/ \sum_{i=1}^{N} (g_i^k)^2 \simeq s^2 \Big/ \sum_{i=1}^{N} (g_i^k)^2, \tag{20}$$

with s^2 given by eqn (17). Since N may not be large (< 10), s^2 may differ significantly from σ^2, and it is better to give a confidence interval for ϵ_k using the known fact (strictly valid only for the linear case) that:

$$(\epsilon - \epsilon_k)/\sigma(\epsilon_k), \tag{21}$$

when σ is estimated from the sample, has the Student t distribution with $N - 1$ degrees of freedom[7]. If α is the probability that $|t|$ based on $N - 1$ d.f. is larger than t_α, we may write the $1 - \alpha$ confidence interval for ϵ_k as $\epsilon_k \pm t_\alpha \sigma(\epsilon_k)$; since λ_k has been regarded as a non-random variable, the corresponding confidence interval for $\hat{\lambda} = \lambda_k + \epsilon_k$ is $\hat{\lambda} \pm t_\alpha \sigma(\epsilon_k)$. From this result, being $\delta L = -1/\lambda^2 \delta\lambda$, we can give the $1 - \alpha$ confidence interval for $\hat{L}$ as $\hat{L} \pm \hat{L}^2 t_\alpha \sigma(\epsilon_k)$.

3. APPLICATION TO EXPERIMENTAL DATA

In the approximate expression of eqn (9), the form of the function $\eta_0(R)$ is still unspecified and actually depends through $\Lambda(\zeta)$ on the semiconductor being considered [see eqn (6)]. We analyze here published measurements on GaAs and Si; since the analytical expressions for $\Lambda(\zeta)$ of GaAs and Si are different, it is convenient to discuss the two cases separately.

3.1. Measurements on GaAs

For GaAs the function $\Lambda(\zeta)$ has the form[2]:

$$\Lambda(\zeta) = A \exp[-(\zeta - \zeta_0)^2/\Delta\zeta^2] - B \exp(-\beta\zeta), \tag{22}$$

with $\zeta_0 = 0.125$, $\Delta\zeta = 0.350$, $\beta = 32$, $B/A = 0.4$; the normalization condition for Λ yields $A = 2.3948$, $B = 0.9579$. From the expressions of Ref. [2], or directly from eqn (6), we have:

$$\eta_0(\rho) = \tfrac{1}{2}A\sqrt{\pi}\Delta\zeta F(\rho) - B/(\beta + \rho), \quad (23)$$

where $\rho = R/L$, and

$$F(\rho) = \exp[-\rho\zeta_0 + (\rho\Delta\zeta/2)^2] \times \operatorname{erfc}(\rho\Delta\zeta/2 - \zeta_0/\Delta\zeta). \quad (24)$$

As suggested in Ref.[2], for the purpose of evaluating numerically $F(\rho)$, it is convenient to use the asymptotic expansion of the erfc function[10] when its argument is large and positive. We will also need the derivative of η_0:

$$\frac{d\eta_0}{d\rho} = A\frac{\sqrt{\pi}}{4}\Delta\zeta(\rho\Delta\zeta^2 - 2\zeta_0)F(\rho) - \tfrac{1}{2}A\Delta\zeta^2\exp[-(\zeta_0/\Delta\zeta)^2] + B/(\beta + \rho)^2. \quad (25)$$

Figure 2 is a semilogarithmic plot of $\eta_0(R/L)$ vs R for various L; the upper horizontal axis has been labelled with the corresponding values of E in GaAs, according to the relation $R = 0.0148\,E^{1.7}$ (R in μm, E in keV)[2]. A similar plot, possibly with smaller steps in L, can be used to estimate rapidly L with the graphical procedure described in Section 2.1.

Figure 2 shows that for large L the plot approaches a straight line; the limit value of the slope of this line can be obtained by developing in powers of ρ the exponential in eqn (6) and integrating term-by-term:

$$\eta_0(\rho) = 1 - \mu_1\rho + \mu_2\rho^2/2 - \ldots, \quad (26)$$

where

$$\mu_k = \int_0^\infty \zeta^k \Lambda(\zeta)\,d\zeta; \quad k = 0, 1, 2, \ldots \quad (27)$$

is the moment of Λ of order k, being $\mu_0 = 1$ since Λ is normalized; a numerical evaluation yields $\mu_1 = 0.257$, $\mu_2 = 0.0952$. To the first order of ρ we also have:

$$\ln \eta_0(\rho) \simeq -\mu_1\rho. \quad (28)$$

Hence we see that for $\rho = R/L \ll 1$ the semilogarithmic plot of η_0 vs R is a straight line with slope μ_1/L; this result can be stated equivalently by saying that in the above limit the extended generation $\Lambda(\zeta)$ is equivalent to unit a point source at a depth $z = \mu_1 R$, since for this source $\eta_0 = \exp(-z/L)$. This property, however, is useful in practice only for large L, since for small L the condition $R/L \ll 1$ can be met only near the origin, where the basic assumption $R \gg h + W$ may not hold.

†The asymptotic expansion of $\eta_0(\rho)$ relies on the fact that in eqn (6) for large ρ, $\exp(-\rho\zeta)$ changes much more rapidly than $\Lambda(\zeta)$ near $\zeta = 0$. This property does not hold for the second term of eqn (22), because of the large value of $\beta = 32$; however, the contribution of this term to η_0 can be evaluated exactly. Hence $\eta_0 \sim \Lambda_1(0)/\rho - 0.96/(32 + \rho)$, where $\Lambda_1(0) = 2.1$ is the value at $\zeta = 0$ of the first (Gaussian) term of eqn (22). This explains why the product $\rho\eta_0(\rho)$ for large ρ is $\simeq 2$ and not $\simeq \Lambda(0) = 1.15$.

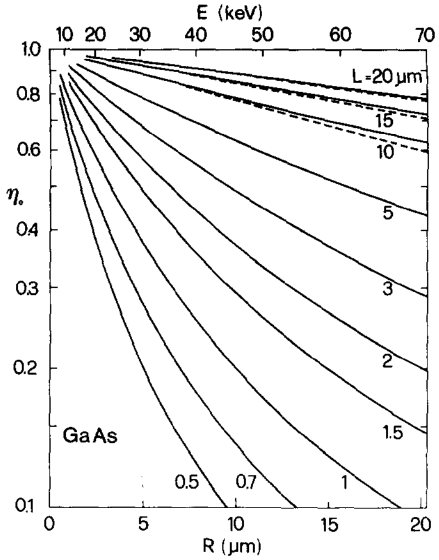

Fig. 2. Theoretical charge-collection efficiency η_0 for an ideal Schottky barrier on GaAs as a function of the range R of primary electrons, for various diffusion lengths L. Dashed lines correspond to the approximation of eqn (28).

To analyze the curves of Fig. 2 in the opposite case of $\rho \gg 1$, it is useful to recall that $\eta_0(\rho) \propto 1/\rho$ for large ρ [see the derivation of eqn (8)]. This result suggests that a plot of $R\eta_0$ vs R should become approximately constant for large R, the value of this constant being proportional to L†. The plots of Fig. 3 confirm this expectation; in addition, we see that the function $R\eta_0(R/L)$ has a broad maximum at $R/L = 10$, with a maximum value close to $2L$. This property can be used to evaluate rapidly small values of L, as will be explained shortly.

3.2. *Experiments by Wu and Wittry[2]*

Wu and Wittry[2] published a number of collection efficiency profiles obtained on Au/GaAs Schottky diodes. The profiles to be analyzed here have been selected so as to cover the widest range of diffusion lengths; the parameters of the corresponding diodes, as given in Ref. [2], are listed in Table 1. Collection efficiency data have been obtained by measuring as accurately as possible from their graphs, and converting the original $\eta(E)$ profiles to $\eta(R)$ by using the known range-energy relation mentioned in Section

Table 1. Parameters of some Au/GaAs Schottky diodes investigated in Ref. [2] and comparison with the values of L obtained in the present study. The equivalent metal thickness is here $h_{eq} = h\rho_m/\rho_s$[2], where ρ_m and ρ_s are the densities of the metal and semiconductor, respectively. The other symbols are defined in the text

h (nm) expt.	h_{eq} (nm)	W (μm)	L (μm) Ref. [2]	L (μm) this study
10	36	0.03	0.41	0.40 ± 0.02
25	91	0.1	0.64	0.64 ± 0.02
11	40	0.06	1.1	1.10 ± 0.03
25	91	0.15	1.7	1.67 ± 0.06
9	33	0.22	4	3.8 ± 0.15
13	47	0.4	12.2	12.2 ± 0.6

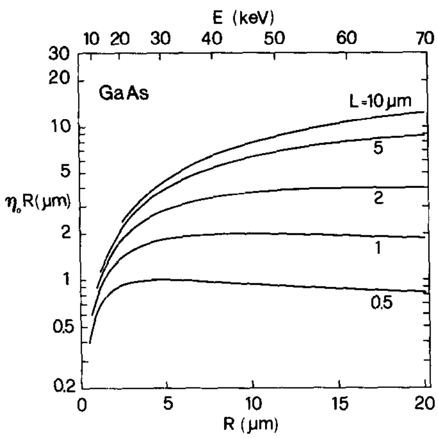

Fig. 3. Plot of the function $R\eta_0$ vs R for different values of L, as calculated from eqns (23) and (24) for GaAs.

3.1. In consideration of the theoretical trends of Fig. 2, only the decreasing, high-energy part of the 6 selected profiles has been considered, and the corresponding experimental points have been plotted in Fig. 4. The curves drawn through the experimental points are the best-fit theoretical curves; the values of L and the related errors have been obtained with the fitting procedure described in Section 2.2. Only a few iterations were required to reach a stable value of L. The errors have been calculated by assuming $\alpha = 0.1$, i.e. by establishing a 90% confidence level for L. Although the absolute error of L increases with L, the relative error is seen to be fairly constant, ranging from 3 to 5%. There may be some uncertainty whether some of the first points of the plots of Fig. 4 should be included in the fit; a simple criterion is to disregard a point at low R if its inclusion changes significantly (i.e. more than the error) the value of L obtained by fitting the remaining points.

The present results and those obtained in Ref. [2] by fitting the whole profiles are compared in Table 1. The agreement is good, the largest difference (about 5%) being observed in the sample with $L = 4\,\mu$m. Following the discussion of the previous section, the profile with $L = 12\,\mu$m also has been fitted using the approximation of eqn (28) for η_0; the resulting value $L = 13 \pm 0.5\,\mu$m indicates that in this case the approximation is adequate.

Now that L has been determined, we can rewrite eqn (9) as

$$\eta \exp(-W/L) = \eta_0(R/L), \tag{29}$$

and evaluate its left-hand side for the experimental points of Fig. 4. A plot of the resulting values vs R/L, according to eqn (29), is expected to fall on the single curve $\eta_0(R/L)$; this property, which is demonstrated clearly by the plot of Fig. 5, is a direct consequence of the possibility of representing the generation function at different electron beam energies by a unique function $\Lambda(z/R)$: the scaling property of Λ is reflected in a similar property of η_0, according to the basic relation (6).

A plot similar to that of Fig. 5, but for the function $(R/L)\eta_0(R/L)$, is shown in Fig. 6. The experimental points reach the maximum of $\rho\eta_0(\rho)$, which occurs at $\rho \simeq 10$, only for shorter diffusion lengths; in fact, since here $R_{max} = R(70\text{ keV}) = 20\,\mu$m, the maximum will fall in the experimental range of values of R only if $L < R_{max}/10 = 2\,\mu$m (see Fig. 3).

This result shows that it is possible to estimate quickly values of L less than $2\,\mu$m by plotting $R\eta$ vs R; the value of the local maximum of $R\eta$, granting that this maximum is present in the plot, is $2L\exp(W/L)$, since that of $R\eta_0$ is $2L$. Hence L can

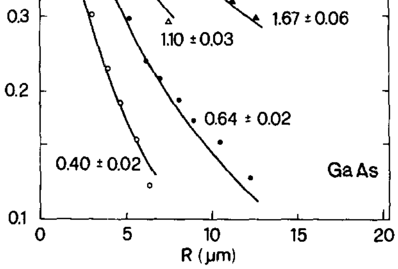

Fig. 4. Selected collection efficiency data obtained in Ref. [2] on Au/GaAs Schottky diodes; refer to Table 1 for the diode parameters. The data have been fitted with eqn (13) for known W; the best-fit values of L and related errors (90% confidence intervals) are given on each curve.

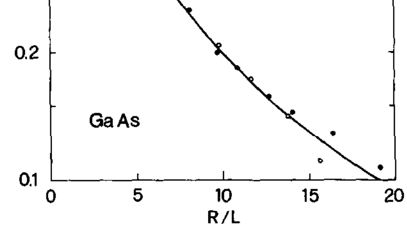

Fig. 5. Comparison between the function $\eta_0(R/L)$ for GaAs and its "experimental" values, as calculated using the data of Fig. 4 and eqn (29). Some of the data for $L = 12.2\,\mu$m have been omitted to improve the readability of the plot.

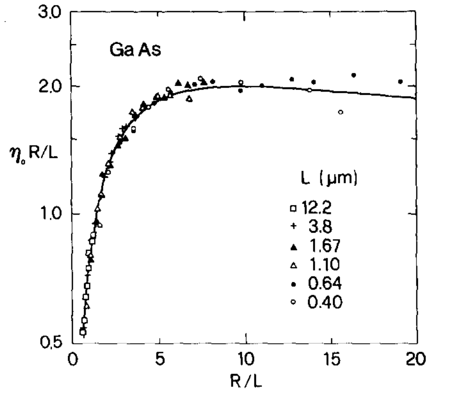

Fig. 6. Comparison between the universal function $(R/L)\eta_0(R/L)$ and its "experimental" values.

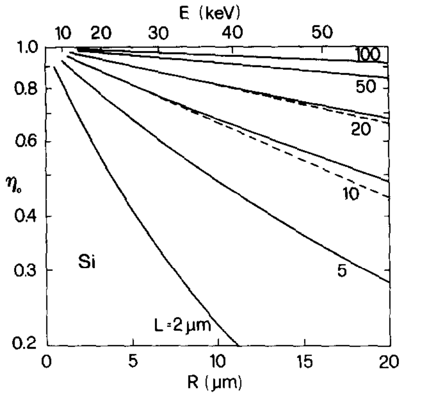

Fig. 7. Theoretical charge-collection efficiency for an ideal Schottky barrier on Si as a function of the range R of primary electrons, for various diffusion lengths L. Dashed lines correspond to the approximation of eqn (28) with $\mu_1 = 0.41$; for $L > 50\,\mu$m the dashed and continuous curves are practically indistinguishable.

be found by solving numerically the simple transcendental equation:

$$L \exp(W/L) = \tfrac{1}{2}(R\eta)_{max}, \quad (30)$$

where W, as before, is assumed to be known. If the maximum available energy of primary electrons is less than 70 keV, the maximum L that can be determined by this method will be reduced accordingly.

3.3. *Measurements on Si*

For silicon, the function $\Lambda(\zeta)$ has been given by Everhart and Hoff[6] in form of a third-degree polynomial:

$$\begin{aligned}\Lambda(\zeta) &= 0.6 + 6.21\zeta - 12.54\zeta^2 + 5.69\zeta^3; \quad 0 \leqslant \zeta \leqslant 1.1 \\ &= 0 \qquad\qquad \zeta > 1.1\end{aligned} \quad (31)$$

The integration required to evaluate η_0 [see eqn (6)] can be performed analytically; however, for numerical computations, especially for large L, it is more convenient to develop $\exp(-\rho\zeta)$ in power series and write:

$$\eta_0(\rho) = \sum_{k=0}^{\infty} \frac{(-1)^k}{k!} \rho^k \int_0^{1.1} \Lambda(\zeta)\zeta^k \, d\zeta. \quad (32)$$

This series involves the moments of Λ [see eqn (27)], which can be easily expressed analytically. Analogously, we have:

$$\frac{d\eta_0}{d\rho} = -\sum_{k=0}^{\infty} \frac{(-1)^k}{k!} \rho^k \int_0^{1.1} \Lambda(\zeta)\zeta^{k+1} \, d\zeta. \quad (33)$$

Figure 7 is a semilogarithmic plot of η_0 vs R for various L; the upper horizontal axis is labelled with the corresponding values of E in Si, according to the relation by Everhart and Hoff[6] $R = 0.0171\ E^{1.75}$ (R in μm, E in keV), which has been extrapolated here up to 56 keV. The curves have been drawn for larger values of L than in the corresponding Fig. 2 for GaAs, since diffusion lengths in Si are usually substantially larger than in GaAs. For large L the plot of Fig. 7 approaches a straight line with reciprocal slope $\mu_1/L = 0.41/L$.

Numerical calculations show that the function $\rho\eta_0(\rho)$ has a maximum value of 1.1, which occurs at $\rho \simeq 5$; therefore a relative maximum will appear in the plot of $R\eta_0$ vs R with $R_{max} = 15\,\mu$m only for $L < 3\,\mu$m. This is a rather small value for Si, so that the method of evaluating L from the maximum of $R\eta$ (see Section 3.2) will be here less useful than in the case of GaAs.

3.4. *Experiments by Kittler et al.[11,12]*

Some collection efficiency profiles published by Kittler *et al.*[11,12] on Al/Si Schottky diodes have been analyzed as done in Section 3.2 for GaAs. The relevant parameters of the four selected diodes are summarized in Table 2. Figure 8 shows the decreasing part of the related $\eta(R)$ profiles, with the experimental points and the best-fit (with known W) theoretical curve. As in Fig. 4, larger values of L are seen to be affected by larger errors, but the relative error ranges again between 2–5%. The present evaluations of L and those of Refs [11,12] are compared in Table 2: for short diffusion lengths the results are practically coincident, but for large L a maximum difference of about 15% is observed. This is most probably related to the known difficulty of determining with precision diffusion lengths larger than the electron range at the maximum energy available[2]. The profiles with $L = 21.8\,\mu$m and $L = 33\,\mu$m could be fitted equally well using the approximation $\eta_0 = \exp(-0.41\ R/L)$, obtaining $L = 22\,\mu$m and $L = 34\,\mu$m, respectively.

Table 2. Parameters of some Al/Si Schottky diodes investigated in Refs [11,12] and comparison with the values of L obtained in the present study. For Al on Si $h_{eq} \simeq h$

h (nm)	W (μm)	L (μm) Refs [11,12]		L (μm) this study
50	0.15	6.5	Ref. [11]	6.6 ± 0.2
140	0.76	7.7		7.7 ± 0.4
100	0.4	24	Ref. [12]	21.8 ± 0.4
100	0.4	38		33 ± 1

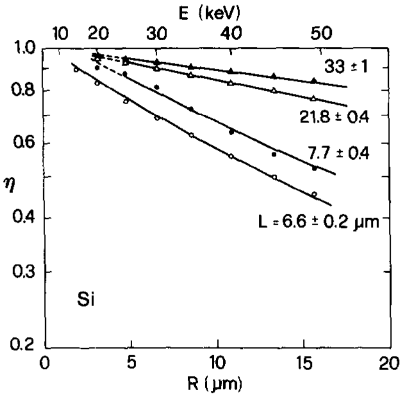

Fig. 8. Selected collection efficiency data obtained in Refs [11, 12] on Al/Si Schottky diodes; refer to Table 2 for the diode parameters. The fitting procedure and the meaning of the errors are the same as in Fig. 4.

Using the experimental data of Fig. 8 and the best-fit values of L, the values of $\eta \exp(-W/L)$ have been computed and are plotted vs R/L in Fig. 9. According to eqn (29) and the related discussion, the plotted points are expected to follow the universal curve $\eta_0(R/L)$ for Si; Fig. 9 confirms this expectation. As in the case of GaAs, the scaling property demonstrated in Fig. 9 is a consequence of the functional dependence of the generation function on $\zeta = z/R$ [see eqn (31)].

4. DISCUSSION AND CONCLUSIONS

The method proposed here to analyze energy-dependent collection efficiency measurements has some analogy with the procedures that have been suggested for evaluating induced current profiles at fixed beam energy[13–15]. The modelling of these experiments generally leads to rather unwieldy expressions for the induced current as a function of the beam-collector distance x_0; therefore, for application purposes, simplified expressions have been derived for $x_0 \gg L$, i.e. for the condition where the generation region is more than a few diffusion lengths away from the junction.

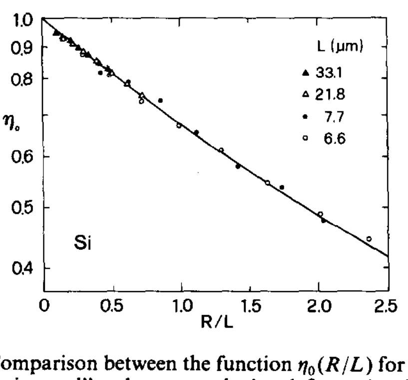

Fig. 9. Comparison between the function $\eta_0(R/L)$ for Si and its "experimental" values, as calculated from the data of Fig. 8 and eqn (29).

In the geometry of interest here, a large (average) distance between the generation region and the junction edge corresponds to high beam energies; this suggested examining the possible simplifications of the general expression for η in the limit of large R. The resulting eqn (9) [eqn (11) is essentially the same] holds for this condition, although here R is only required to be large in comparison to $h + W$ and not to L. The simplified expression (9) has the advantage of approximating the profile $\eta(R)$ of an actual device in terms of the function $\eta_0(R/L)$ of an ideal surface barrier; moreover, eqn (9) does not contain the metal thickness h and the second geometrical parameter W appears through a simple exponential factor. This latter circumstance suggested the possibility of an easy graphical analysis of the collection efficiency data.

By examining the behaviour of $\eta_0(R/L)$ in the two limiting cases where R is either much smaller or much larger than L, it has been found that the diffusion length determines the slope of the plot of $\ln \eta$ vs R for $R/L \ll 1$; in the opposite case of $R/L \gg 1$, where the slope changes continuously (see Figs 2 and 7), the value of L was shown to be related to a different property of $\eta(R)$, i.e. to the maximum value of the product $R\eta(R)$.

In addition, the closed form expressions for η_0 and $d\eta_0/d\rho$ (and hence for η and $\partial\eta/\partial\lambda$) simplified the non-linear numerical fitting required to determine L, and also allowed a specification of the statistical error of this determination, an information that is usually not given. The present estimates of L and those obtained by fitting the whole $\eta(E)$ profile are generally within this error for L less than about $10\,\mu$m. Nevertheless, it remains difficult to assess the absolute accuracy of this determination since, for instance, the values of L obtained by the electron injection method considered here seem to be systematically smaller than those obtained by optical excitation on the same samples[3,11].

Acknowledgement—This work was performed with a partial contribution of CNR-Progetto Finalizzato "Materiali e Dispositivi per l'Elettronica a Stato Solido".

REFERENCES

1. H. J. Leamy, *J. appl. Phys.* **53,** R51 (1982).
2. C. J. Wu and D. B. Wittry, *J. appl. Phys.* **49,** 2827 (1978).
3. L. Tarricone, C. Frigeri, E. Gombia and L. Zanotti, *J. appl. Phys.* **60,** 1745 (1986).
4. M. Kittler and K. W. Schröder, *Physica Status Solidi* **77a,** 139 (1983).
5. G. E. Possin and C. G. Kirkpatrick, *Scanning Electron Microscopy/1979/I*, p. 245 (Edited by O. Johari). SEM Inc, AMF O'Hare (1979).
6. T. E. Everhart and P. H. Hoff, *J. appl. Phys.* **42,** 5837 (1971).
7. G. H. Winslow, in *Techniques of Metals Research*, Vol. VII, part I (Edited by R. F. Bunshah), p. 448. Wiley, New York. (1972).

8. W. J. Kennedy Jr and J. E. Gentle, *Statistical Computing*, Chap. 10.3. M. Dekker, New York (1980).
9. A. G. Frodesen, O. Skjeggestad and H. Tøfte, *Probability and Statistics in Particle Physics*, Chap. 10.8. Universitetsforlaget, Oslo (1979).
10. M. Abramowitz and I. A. Stegun, *Handbook of Mathematical Functions*, p. 298. Dover, New York (1965).
11. M. Kittler, W. Seifert, K. W. Schröder and E. Susi, *Cryst. Res. Tech.* **20,** 1453 (1985).
12. M. Kittler, W. Seifert, K. Schmalz and K. Tittelbach-Helmrich, *Physica Status Solidi* **96a,** K133 (1986).
13. F . Berz and H. K. Kuiken, *Solid-St. Electron.* **19,** 437 (1976).
14. D. E. Ioannou and C. A. Dimitriadis, *IEEE Trans. Electron Dev.* **ED-29,** 445 (1982).
15. H. K. Kuiken and C. van Opdorp, *J. appl. Phys.* **57,** 2077 (1985).